Progress In Electromagnetics Research C, Vol. 129, 63–72, 2023

Microstrip Fed Pi-Slot Patch Antenna with T-Slot DGS for UWB Applications

Shaik Jabeen[1, *] and Gumireddy Hemalatha[2]

Abstract—An ultra-wideband microstrip fed patch antenna with a defective ground surface is presented in this paper. The above-mentioned antenna comprises a T-slot in the ground plane and a Pi-slot in a rectangular patch. The proposed antenna is developed and modeled using the High-Frequency Structure Simulation tool on an RTDuroid 5880 substrate with a thickness of 1.6 mm and a dielectric constant of 2.2. A T-shaped defect is carved in the ground plane to enhance the antenna's radiation properties, gain, and bandwidth. A conventional Pi-slotted patch antenna operating at 9.74 GHz with a return loss of 19.7 dB is designed, followed by an ultra-wideband antenna embedded with a T-slot in the partial ground surface operating from 7.15 GHz to 10.925 GHz with an impedance bandwidth ($S_{11} < -10$ dB) of 3.775 GHz. It showcases exceptional characteristics with a peak gain of 6.99 dBi at 8.95 GHz. A satisfactory agreement is found between the experimental data and simulation results. The proposed Pi-slot patch antenna with the defective ground has applications in radar, satellite, weather monitoring, and vehicle speed detection for law enforcement.

1. INTRODUCTION

Antennas with low cost, effective performance, small size, wide bandwidth, and low profile typically meet the requirements of modern wireless communication systems [1]. The availability of effective, small, and portable devices with fast data rates and low signal power is essential for everyday communication. Microstrip patch antenna [2] has drawbacks, including a small bandwidth and low gain. RF designer's main objective is to reduce the antenna's physical size while maintaining excellent performance. A miniaturized antenna emerges due to the continuous development of wireless communication [3]. Modern wireless communication networks offer services that support several standards and mobile cellular systems like GSM, UMTS, WLAN, Wi-Fi, Wi-MAX, LTE, Bluetooth, etc. It has been proposed that stacking, different feeding techniques, Frequency Selective Surfaces (FSS), Electromagnetic Band Gap (EBG), Photonic Band Gap (PBG), Metamaterial, Defected Ground Structure (DGS), and other technologies can improve the characteristics of traditional Microstrip antennas [4]. Etched slots or defects on the ground plane of Microstrip circuits are referred to as defective ground structures. The shielded current distribution will be disturbed by the flaws etched on the ground plane, leading to controlled excitation and electromagnetic wave propagation through the substrate layer. Compared to a standard patch antenna of the same physical length, the patch antenna with a defective ground structure has a significantly longer electric length [5].

DGS unit and periodic DGS are different aspects for utilizing DGS performance. In the literature, numerous shapes of geometries implanted on the ground plane under the microstrip line have been documented [6–9]. Rectangular dumbbells, circular dumbbells, spirals, "U," "V," "H," cross, and concentric rings are examples of these shapes. DGS has also been used to make wideband and

Received 28 November 2022, Accepted 12 January 2023, Scheduled 26 January 2023
* Corresponding author: Shaik Jabeen, Research Scholar (sjabeen24@gmail.com).
[1] Jawaharlal Nehru Technological University Anantapur, Ananthapuramu, India. [2] K.S.R.M. College of Engineering, Kadapa, Affiliated to Jawaharlal Nehru Technological University Anantapur, Ananthapuramu, India.

ultra-wideband (UWB) microstrip antennas. To increase the bandwidth of the microstrip antenna, a square-shaped flaw has been integrated on the ground plane with an open-terminated microstrip line [10]. In [11], periodic structures for planar transmission lines, including PBG and DGS, have created considerable interest due to their wide range applications in antennas and microwave circuits. DGS units are etched away periodically in different aspects to maximise DGS performance. The increased slow-wave impact and additional equivalent elements are significant periodic structure qualities that can be attained and used to reduce circuit dimensions. Periodic DGSs are concerned with characteristics such as the geometry of the unit DGS, the distance between the DGS units, and the distribution of the different DGSs.

The frequency range from 3.1 GHz to 10.6 GHz was allocated to commercial UWB applications by the Federal Communication Commission (FCC). In [12], UWB systems' impending widespread commercial deployment has revived interest in the area of UWB antennas. It is widely known that the limited bandwidth and moderate gain of a standard microstrip antenna confine its application in contemporary UWB communication systems. Due to the constrained area inside the small wireless terminal, installing numerous antennas for multiple working frequencies is challenging. Researchers recently developed various new antennas to address these issues, including reconfigurable, UWB, and multiband antennas.

Yadav et al. [13] demonstrated a compact rectangular slot antenna with a ladder structure of size $14 \times 18 \times 1.6\,\text{mm}^3$, developed in the UWB. The slot antenna has a partial ground plane with rectangular slots resonating from 3.1 to 11.8 GHz and has a maximum gain of 2.2 dB with a maximum radiation efficiency of 69%. This antenna configuration is used in 3.5–5.5 GHz (WiMAX), 5.2–5.8 GHz (WLAN), and other wireless communication applications.

Suvarna et al. [14] constructed a miniaturised antenna with a Koch fractal defective ground structure (KFDGS) for C/X- and Ku-bands. The tri-band miniaturised antenna operates at 6.35, 9.05, and 13.05 GHz with return losses of 22.41, 25.05, and 28.54 dB, respectively. Peak directivity and gain of 3.07 and 2.80 dBi at 6.35 GHz, 4.78 and 4.65 dBi at 9 GHz, and 7.73 and 7.76 dBi at 13.05 GHz, respectively, were obtained for the miniaturised antenna.

Khoiro and Firdaus [15] developed a microstrip triple-band antenna with a "T"-shaped strip and a dumbbell DGS for wireless communication. The antenna can resonate at three frequencies: 2.35 GHz, 3.20 GHz, and 5.88 GHz, which cover the frequency spectrum standard for WLAN and WiMAX applications. This antenna's features include its small size, simple design, three resonant frequencies, and reasonable gain of 2.3, 1.79, and 4.22, respectively.

The developed antenna is used for UWB applications and operates in the 7.15 GHz–10.925 GHz frequency range. Applications for UWB antennas have expanded to cover a wide range of computing devices and Internet of Things (IoT) peripherals. A UWB antenna is used in majority of these wireless communication systems for data transmission, reception, positioning, location identification, sensing, and tracking. UWB technology's unique characteristics, such as its fast data rate, wide bandwidth, low cost, and low power consumption, make it excellent for recording extremely accurate spatial and directional data. UWB technology is intrinsically more exact in locating devices or objects than Wi-Fi or Bluetooth, increasing the applications of smart devices and contributing to the development of interconnected smart systems and the IoT.

This article develops a rectangular patch antenna with a Pi-slot embedded with a T-slot in the partial ground plane. Despite its less compact form, the proposed antenna displays a measured gain of 6.99 dB at 8.95 GHz for UWB applications. DGS-based antennas are noticeably bigger at lower frequencies in Table 1, and the suggested work increases gain. In Table 1, DGS-based antennas are more significant at lower frequencies, and the proposed work improves the gain.

The performance of a microstrip fed Pi slot patch antenna with a T slot DGS for UWB applications has been examined for C-band and X-band frequency ranges in this article. Section 2 explains the proposed antenna's design in detail, including design equations, antenna construction, S_{11} characteristics, and parametric analysis for performance optimization and gain. A Pi slot patch with a T-slot DGS and a measurement setup with vector network analyzer (VNA) and anechoic chamber are included.

Section 3 summarises the simulated and measured data, including the reflection coefficient, voltage standing wave ratio (VSWR), gain, current distribution, and far-field radiation characteristics. Section 4

Table 1. A defective ground structure based antenna analysis.

Ref.	Patch Size (mm^2)	Substrate	Design Description	Operating Frequency Band (GHz)	Maximum Realized Gain (dBi)	Bandwidth (GHz)
[13]	14×18	FR4	A novel rectangular slot antenna with ladder structure & DGS	3.1 to 11.8	2.2	8.7
[14]	8×5.86	Roger RT Duroid	A miniaturized antenna with a Koch fractal-defected ground structure	6.22 to 6.44, 8.92 to 9.05, and 12.92 to 13.20	2.80, 4.65 and 7.76	0.22, 0.13 and 0.28
[15]	17×15.5	FR4	A Microstrip Triple-band Antenna with T-strip and Dumbbell DGS	2.17–2.51, 2.93–3.40 and 5.42–6.17	2.3, 1.79 and 4.22	0.34, 0.47 and 0.75

brings the work covered in this paper to a conclusion.

2. DEVELOPED ANTENNA DESIGN AND DISCUSSION

Ansys HFSS V 15.0 is used to create an ultra-wideband antenna. Figures 1(a) and 1(b) show the front and rear views of the proposed antenna arrangement, which is excited by a lambda/2 feeder and has a T-slot DGS etched on the ground plane. The optimized geometrical dimensions of the developed antenna are given in Table 2. The substrate utilized is Roger RT Duroid 5880, which has a dielectric permittivity of 2.2, a height of 1.6 mm, and a layout of $70 \times 50\,mm^2$. It operates between 7.15 GHz and 10.925 GHz and resonates at 8.95 GHz. Periodic or non-periodic structures detached from the ground plane take up minimal space and are easy to build [16].

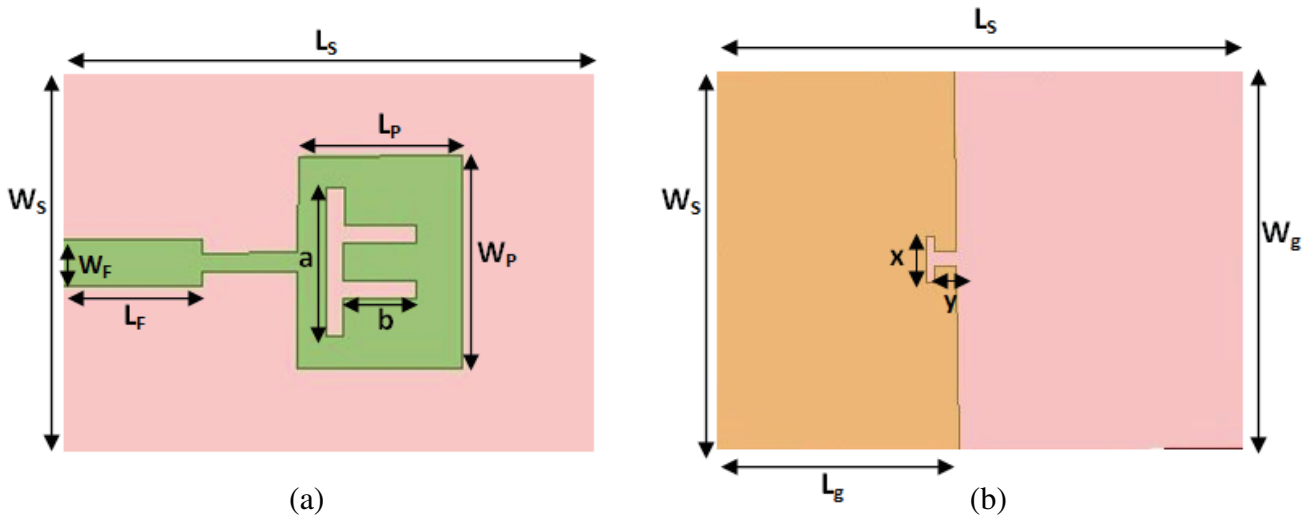

Figure 1. An Ultra-Wide Band Pi-slot patch antenna with T-slot DGS (a) Top view. (b) Bottom view.

Using Pi-slot geometry on the patch, the current is disturbed. As a result, the resonance frequency is changed by lengthening the electrical length (βl) antenna, which changes the capacitance and inductance values and, in turn, influences the realized gain and resonant frequency [17].

The following mathematical equations are used to determine the proposed antenna's length and width.

Table 2. Geometrical dimensions of a designed Pi-slot antenna with T-slot DGS.

Parameters	Value [mm]	Parameters	Value [mm]
Ground width, W_G and Substrate width, W_S	50	Feed Width, W_f	4.92
Substrate length, L_S	70	Length of feed, L_f	21.08
Ground length, L_G	31.90	Width of Slot, a	16
Patch length, Lp	18.51	Length of Slot, b	8.40
Patch width, Wp	22.40	Width of T-slot DGS, x	6
Substrate thickness, h	1.6	Length of T-slot DGS, y	2.87

The effective dielectric constant is determined using the expression

$$\varepsilon_{reff} = \frac{\varepsilon_r + 1}{2} + \frac{\varepsilon_r - 1}{2\sqrt{1 + 12h/W}} \tag{1}$$

$$\Delta L = 0.412h \frac{(\varepsilon_{reff} + 0.3)\left(\frac{W}{h} + 0.27\right)}{(\varepsilon_{reff} - 0.258)\left(\frac{W}{h} + 0.8\right)} \tag{2}$$

The effective length for a specific f_r is given as

$$L_{eff} = \frac{c}{2f_0\sqrt{\varepsilon}_{reff}} \tag{3}$$

The patch's effective length is expressed as

$$L_P = L + 2\Delta L \tag{4}$$

The patch's effective width is expressed as

$$W_P = \frac{c}{2f_0\sqrt{\frac{\varepsilon_{reff} + 1}{2}}} \tag{5}$$

The designed antenna prototype is built in several steps. Table 3 illustrates the characteristics of constructed antenna at various steps, from case (a) to case (d). In case (a), a rectangular patch with a microstrip feed and a quarter wave transformer is developed to achieve impedance matching. To maximize the gain in case (b), a Pi-slot is incorporated in the rectangular patch. In case (c), a partial ground plane is employed to increase bandwidth and gain. The current distribution is disturbed when

Table 3. Characteristics of the developed antenna with T-Slot DGS at various steps.

Type of antenna design structure	**Resonant frequency (GHz)**	**Return loss (dB)**	**VSWR**	**Band Width (MHz.)**	**Gain (dBi)**
Case-a	8.25	−16.9	1.33	300	7.6
Case-b	9.74	−19.7	1.22	700	8.79
Case-c	8.04	−20.7	1.19	1900	6.34
Case-d (Proposed work)	8.95	−31.4	1.05	3775	6.99

DGS is implemented with a microstrip antenna. The values of the antenna's line inductance and capacitance, which are created as a result of changes in the current distribution, impact the surface current flow and impedance. In the last step, the proposed antenna is constructed with a T-slot loaded in the partial ground surface to achieve wide bandwidth for wireless communication.

The typical rectangular patch antenna has a gain of 7.6 dBi, an impedance bandwidth of 300 MHz, and works at 8.25 GHz. The gain is increased to 8.79 dBi and the impedance bandwidth to 700 MHz at the operating frequency of 9.74 GHz after inserting a Pi-slot into the patch, as illustrated in Figure 2(b). Later, as depicted in Figure 2(c), a partial ground plane causes a 6.34 dB gain reduction, a resonant frequency shift to 8.04 GHz, and an impedance bandwidth changes to 1900 MHz. Figure 2(d) illustrates how the design structure was modified by incorporating a T-slot on the partial ground plane, producing a 6.99 dB gain with a 3775 MHz bandwidth at an 8.95 GHz resonant frequency.

Figures 3(a), (b), (c), and (d) depict simulated parameters such as reflection coefficient, VSWR, and radiation patterns at phi = 0 deg and phi = 90 deg of developed antenna at different steps. The ground plane's length and patch width are changed in parametric analysis. Figure 4 depicts the simulated return

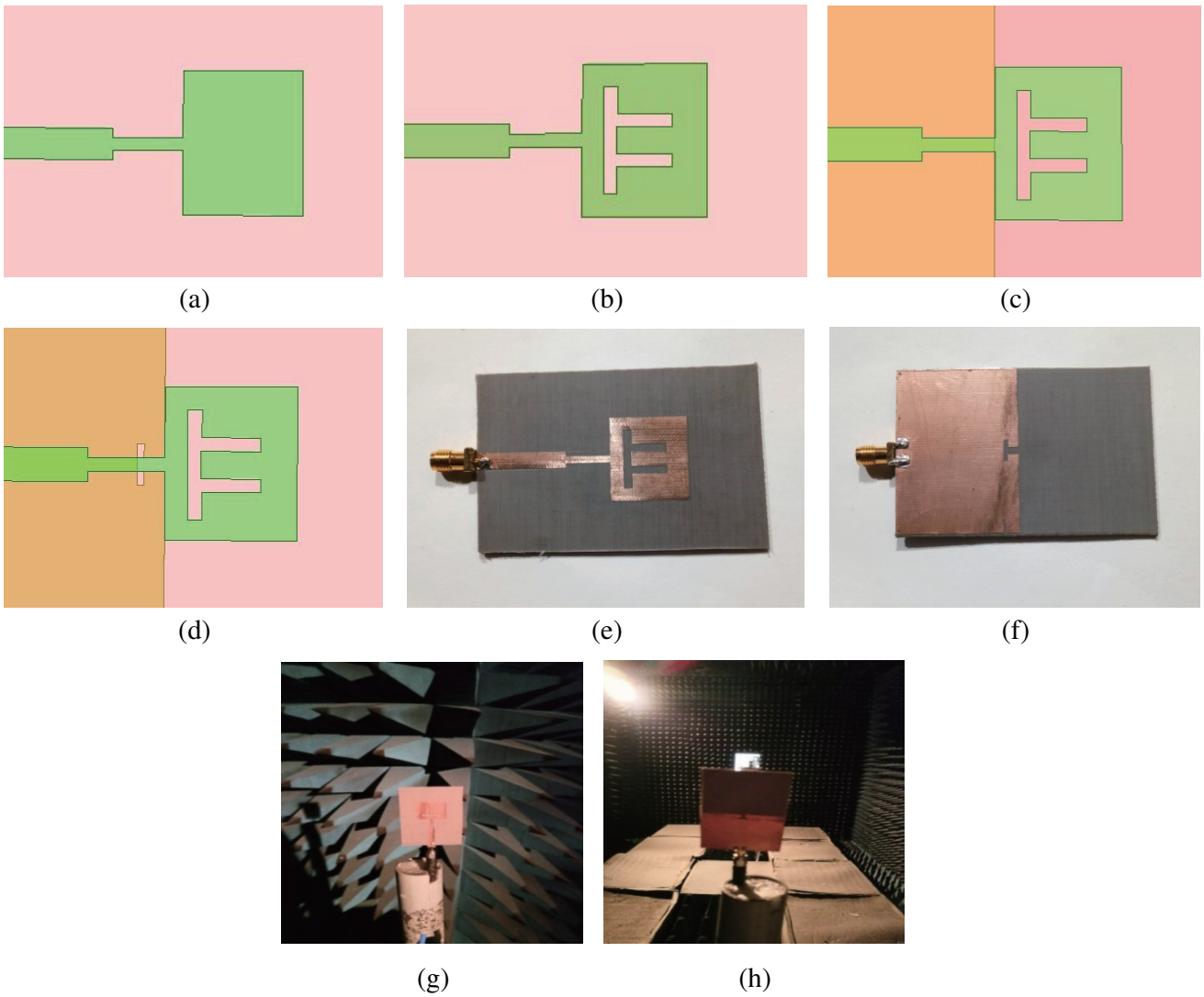

Figure 2. The steps involved in creating a Pi-slot patch antenna with embedded T-slot DGS. (a) Microstrip Fed conventional antenna. (b) Patch with Pi-slot, (c) Patch with pi-slot and partial ground plane. (d) Patch with pi-slot and T-slot on the ground plane. (e) Top view — patch. (f) Bottom view — Ground and (g), (h) Measurement of the developed design in an anechoic chamber.

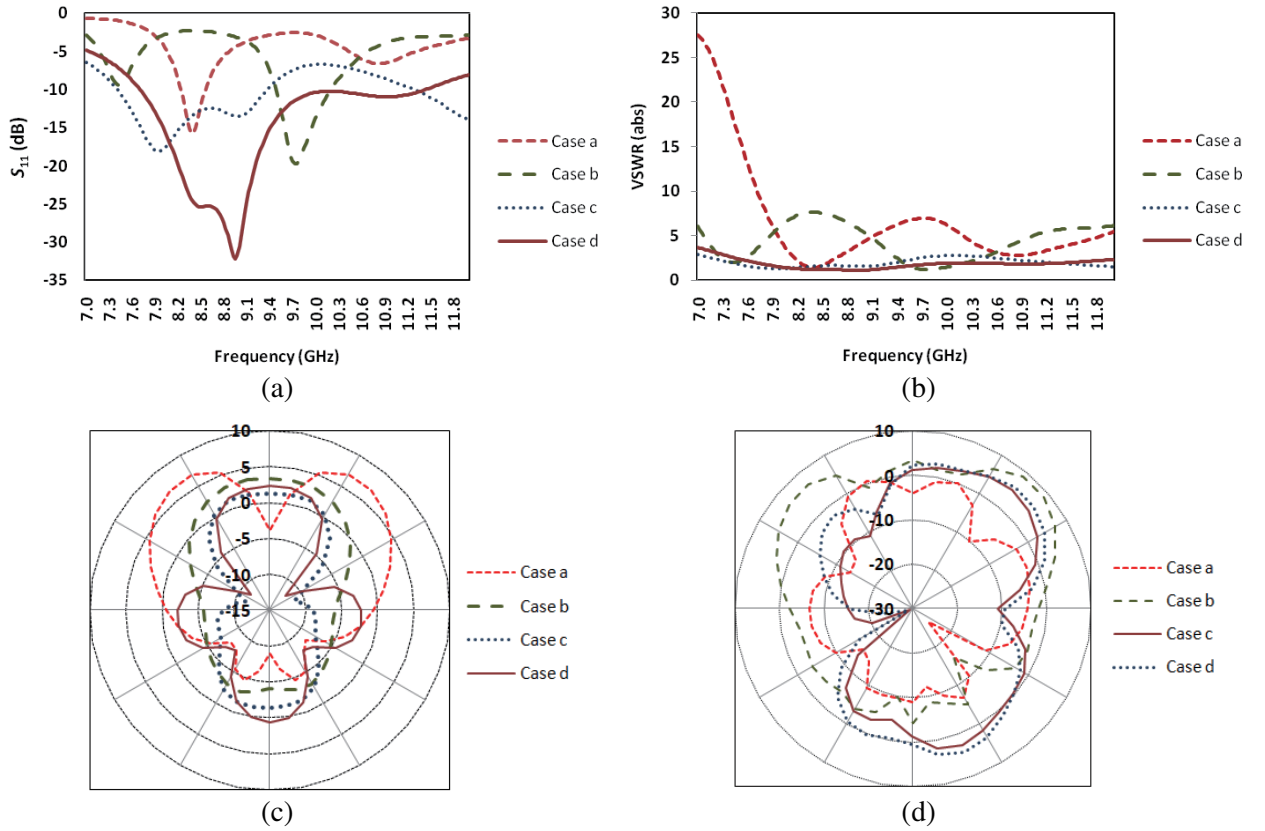

Figure 3. Simulated characteristics of constructed antenna at various steps. (a) Return loss (dB), (b) VSWR, (c) E-plane pattern, (d) H-plane pattern.

loss (S_{11}) obtained by creating a Pi-slot patch with a DGS miniature antenna. Figures 4(a), (b), (c), and (d) show a parametric analysis of various ground plane lengths, patch widths, patch lengths, and substrate lengths, respectively. Due to T-slot DGS and Pi-slot in the patch, resonant frequency moves from right to left. Using an Agilent N5247A vector network analyzer (VNA), the return loss of the pi-slot patch antenna with T-slot DGS is measuredby activating the port with a 50-ohm load impedance. Before this, the VNA is calibrated using the 3.5 SMA calibration kits and the through-reflect-line (TRL) procedure. The proposed antenna functions for S_{11} <-10 dB between 7.15 GHz and 10.925 GHz and achieves a 3.775 GHz impedance bandwidth, which is appropriate for UWB applications.

3. RESULTS AND DISCUSSION

The results for return loss (S_{11}) were examined between measured and simulated values. As shown in Figure 5, the S parameters were determined using a VNA. The measured and simulated return losses and VSWR are plotted with good agreement in Figures 6(a) and (b).

Figure 7 depicts the distribution of current elements on the surface of the designed patch antenna structure at the resonant frequency 8.95 GHz. Furthermore, the newly created current routes caused by the etching slots have introduced additional electrical length, lowering the resonant frequency [18].

The proposed antenna's gain and radiation patterns were measured in an anechoic chamber, as depicted in Figure 2(g). Figures 8(a) and (b) show the simulated radiation patterns in the E plane (phi $= 0°$) and H plane (phi $= 90°$) of a Pi-slot patch antenna with T-slot DGS at 8 GHz and 10 GHz, respectively.

Figures 9(a) and (b) show the simulated and measured radiations in the E plane (phi $= 0°$) and H plane (phi $= 90°$) of a Pi-slot patch antenna with T-slot DGS at 8.95 GHz.

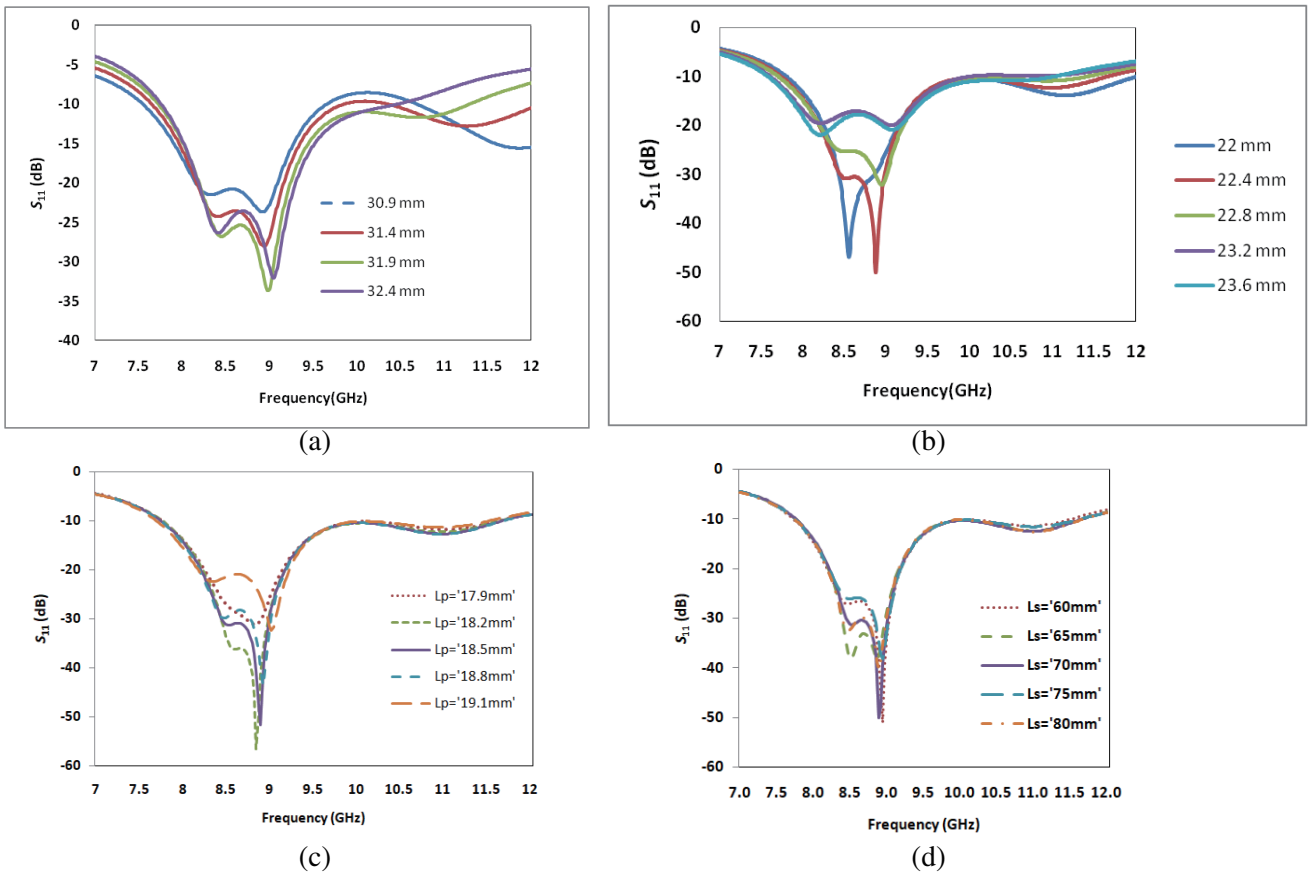

Figure 4. Parametric analysis of the developed antenna, (a) L_G, (b) W_P, (c) L_P, and (d) L_S.

Figure 5. Experimental setup of proposed Pi-slot patch antenna with T-slot DGS.

Figure 10(a) shows a gain polar plot of the proposed antenna, 6.99 dBi at 8.95 GHz, and Figure 10(b) shows the simulated and measured peak gain of a designed antenna at 8.95 GHz. Compared with [13–15], the developed antenna exhibits better gain.

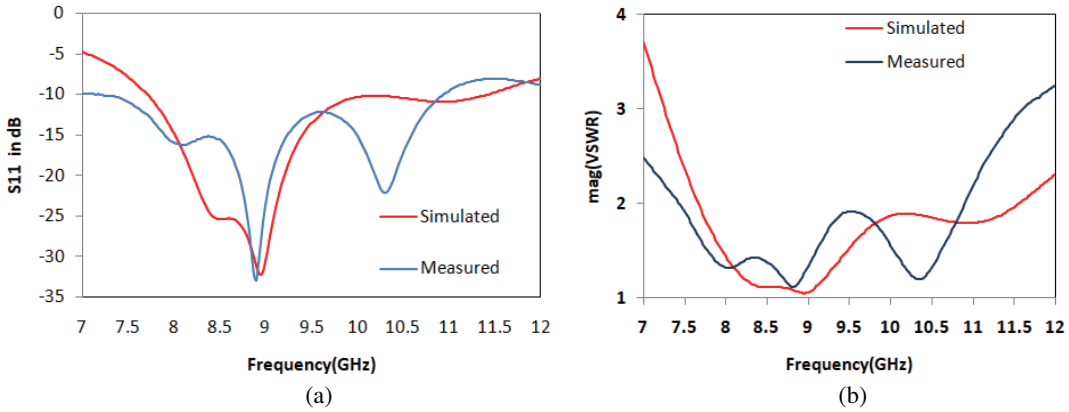

Figure 6. Simulated and measured characteristics of proposed antenna. (a) Return loss, (b) VSWR.

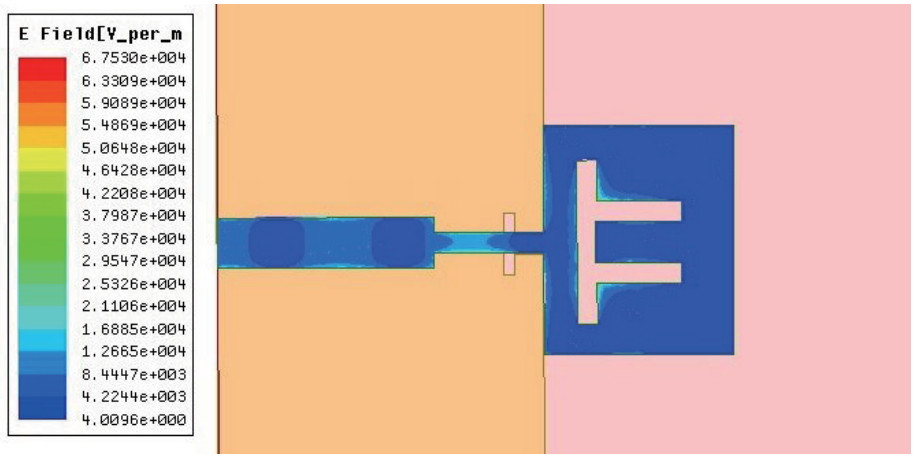

Figure 7. Current distribution of proposed Pi-slot patch antenna with T-slot DGS.

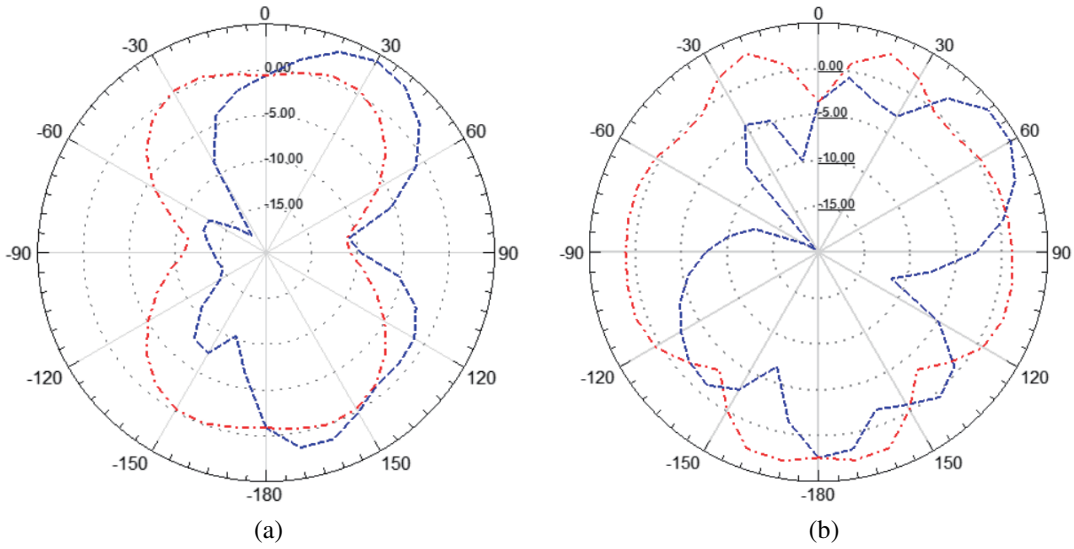

Figure 8. Simulated radiation pattern of pi-slot patch antenna with T-slot DGS at a frequency of (a) 8 GHz (b) 10 GHz.

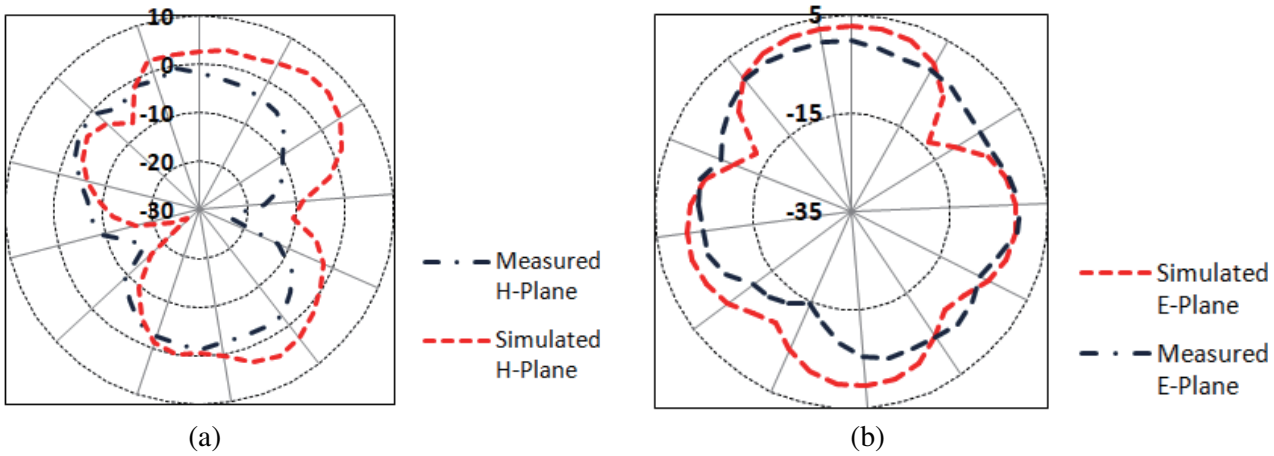

(a) (b)

Figure 9. Measured and simulated radiation patterns of Pi-slot patch antenna with T-slot DGS at a resonant frequency of 8.95 GHz. (a) H plane, (b) E plane.

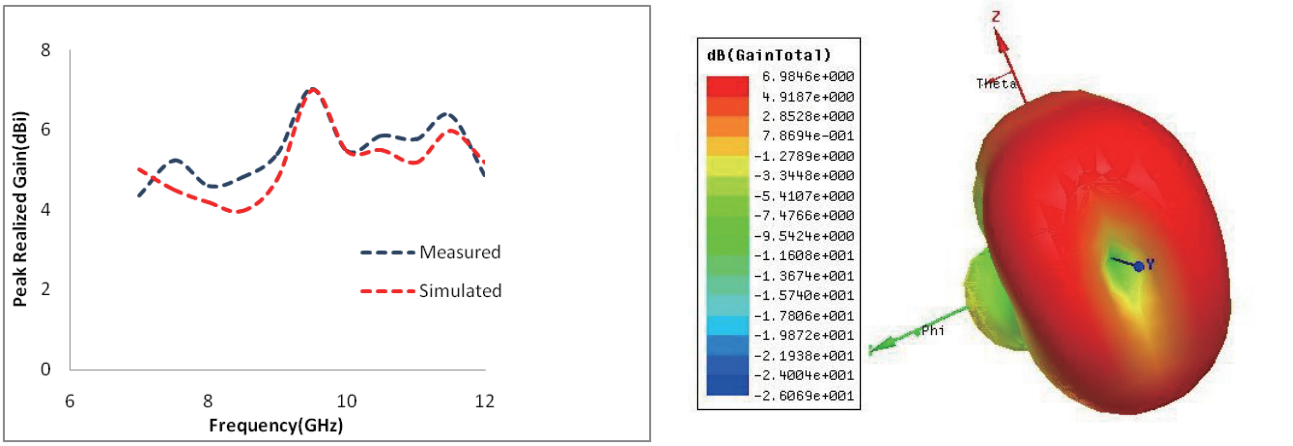

(a) (b)

Figure 10. (a) Simulated and measured gain characteristics of the designed antenna. (b) Gain plot of proposed Pi-slot patch antenna with T-slot DGS at 8.95 GHz.

4. CONCLUSION

This article presents a Microstrip fed Pi-slot patch antenna with T-slot DGS for UWB applications, which operates at 8.95 GHz with an impedance bandwidth from 7.15 to 10.925 GHz, and has return loss (S_{11}) of -31.4 dB. The antenna is $18.51 \times 22.40 \times 1.6\,\text{mm}^3$ in size and is designed on a Roger RT Duroid 5880. It operates with a well-realized peak gain of 6.99 dB. The bandwidth of 3.775 GHz is achieved at 8.95 GHz. Compared with the reference antennas, the developed antenna has better gain. The proposed antenna is suitable for C-band and X-band applications. Good matching between the measured and simulated results is achieved.

REFERENCES

1. Balanis, C. A., "Antenna theory," *Analysis and Design*, 3rd Edition, Wiley, New York, 2005.

2. Garg, R., P. Bhartia, I. Bahl, and A. Ittipiboon, *Microstrip Antenna Design Book*, Artech House, Boston, 2000.
3. Haque, S. K. M. and K. M. Parvez, "Slot antenna miniaturization using slit, strip, and loop loading techniques," *IEEE Transactions on Antennas and Propagation*, Vol. 65, No. 5, 2215–2221, May 2017.
4. Parkash, D. and R. Khanna, "Multiband antenna structure for heterogeneous wireless communication systems using DGS technique," *International Journal of Microwave and Wireless Technologies*, Vol. 6, No. 5, 521–526, 2014.
5. Salgare, D. S. and S. R. Mahadik, "A review of defected ground structure for microstrip antennas," *International Research Journal of Engineering and Technology*, Vol. 2, No. 6, 150–154, 2015.
6. Lim, J.-S., C.-S. Kim, Y.-T. Lee, D. Ahn, and S. Nam, "A spiral-shaped defected ground structure for coplanar waveguide," *IEEE Microwave and Wireless Components Letters*, Vol. 12, No. 9, 330–332, 2002.
7. Boutejdar, A., G. Nadim, S. Amari, and A. S. Omar, "Control of band- stop response of cascaded microstrip low-pass-bandstop filters using arrowhead slots in backside metallic ground plane," *IEEE Antennas and Propagation Society International Symposium*, Vol. 1B, 574–577, 2005.
8. Li, J., J. Chen, Q. Xue, J. Wang, W. Shao, and L. Xue, "Compact microstrip lowpass filter based on defected ground structure and compensated microstrip line," *Proceedings of IEEE MTT-S International Microwave Symposium*, Long Beach, Calif, USA, June 2005.
9. Chen, J.-X., J.-L. Li, K.-C. Wan, and Q. Xue, "Compact quasielliptic function filter based on defected ground structure," *IEEE Proceedings: Microwaves, Antennas and Propagation*, Vol. 153, No. 4, 320–324, 2006.
10. Jan, J.-Y. and J.-W. Su, "Bandwidth enhancement of a printed wide-slot antenna with a rotated slot," *IEEE Transactions on Antennas and Propagation*, Vol. 53, No. 6, 2111–2114, 2005.
11. Weng, L. H., Y. C. Guo, X. W. Shi, and X. Q. Chen, "An overview on defected ground structure," *Progress In Electromagnetics Research B*, Vol. 7, 173–189, 2008.
12. Kurniawan, A. and S. Mukhlishin, "Wideband antenna design and fabrication for modern wireless communications systems," *Science Direct, Procedia Technology*, Vol. 11, 348–353, 2013.
13. Yadav, M. V., S. Baudha, Y. Bansal, and S. K. Verma, "A novel compact rectangular slot antenna with ladder structure for ultra-wideband applications," *Telecommunications and Radio Engineering*, Vol. 81, No. 1, 2022.
14. Suvarna, K., N. Ramamurthy, and D. V. Vardhan, "A tri-band miniaturized antenna using fractal defected ground structure for C/X and Ku-band applications," *Progress In Electromagnetics Research M*, 115–128, 2022.
15. Khoiro, M. and R. A. Firdaus, "A microstrip triple-band antenna with T-strip and dumbbell defected ground structure for wireless applications," *International Joint Conference on Science and Engineering 2021 (IJCSE 2021)*, 429–433, Atlantis Press, 2021.
16. Khandelwal, M. K., B. K. Kanaujia, and S. Kumar, "Defected ground structure: Fundamentals, analysis, and applications in modern wireless trends," *International Journal of Antennas and Propagation*, Vol. 2017, Article ID 2018527, 22pages, 2017.
17. Gopi, D., A. R. Vadaboyina, and J. R. K. Dabbakuti, "DGS based monopole circular-shaped patch antenna for UWB applications," *SN Applied Sciences*, Vol. 3, No. 2, 2021.
18. Ullah, S., C. Ruan, M. S. Sadiq, T. Ul Haq, A. K. Fahad, and W. He, "Super wide band, defected ground structure (DGS), and stepped meander line antenna for WLAN/ISM/WiMAX/UWB and other wireless communication applications," *Sensors*, Vol. 20, No. 6, 1735, 2020.